Estimation of atmospheric particle formation rates through an analytical formula: Validation and application in Hyytiälä and Puijo, Finland

Elham Baranizadeh[1], Tuomo Nieminen[1], Taina Yli-Juuti[1], Markku Kulmala[2], Tuukka Petäjä[2], Ari Leskinen[1,3], Mika Komppula[3], Ari Laaksonen[1,4], Kari E. J. Lehtinen[1,3]

[1]Department of Applied Physics, University of Eastern Finland, Kuopio, Finland

[2]Department of Physics, University of Helsinki, Finland

[3]Finnish Meteorological Institute, Kuopio, Finland

[4]Climate research Unit, Finnish Meteorological Institute, Helsinki, Finland

Correspondence to: Elham Baranizadeh (elham.baranizadeh@gmail.com)

Abstract. The formation rates of 3-nm particles were estimated at SMEAR IV, Puijo (Finland) where the continuous measurements extend only down to 7 nm in diameter. We extrapolated the formation rates at 7 nm (J_7) down to 3 nm (J_3) based on an approximate solution to the aerosol general dynamic equation, assuming a constant condensational growth rate, a power-law size dependent scavenging rate and negligible self-coagulation rate for the nucleation mode particles. To evaluate our method, we first applied it to new-particle formation (NPF) events in Hyytiälä (Finland), which extend down to 3 nm, and, therefore, J_3 and J_7 can be determined directly from the measured size distribution evolution. The Hyytiälä results show that the estimated daily mean J_3 slightly overestimate the observed mean J_3, but a promising 91% of the estimated J_3 are within a factor of 2 from the measured ones. However, when considering detailed daily time evolution, the agreement is not as good due to fluctuations in data as well as uncertainties in estimated growth rates which are required in order to calculate the time-lag between formation of 3-nm and 7-nm particles. At Puijo, the mean J_7 for clear NPF days during April 2007-December 2015 was 0.44 $cm^{-3}s^{-1}$, while the extrapolated mean J_3 was 0.61 $cm^{-3}s^{-1}$.

1 Introduction

Atmospheric new particle formation (NPF) events, i.e. nucleation and subsequent growth of newly formed particles have received increasing attention due to their impact on climate and human health (Kulmala et al., 2004; Merikanto et al., 2009; Nie et al., 2014, Kerminen et al., 2012; Fuzzi et al., 2015, Minguillón et al., 2015 and references therein). Many studies have been conducted to find out which variables cause and which possibly inhibit NPF events. Sulfuric acid, water and ammonia have already long been considered important molecules for atmospheric new particle formation (Weber et al., 1995; Weber et

al., 1996; Korhonen et al., 1999; Kulmala et al., 2000; Laaksonen et al., 2008; Xiao et al., 2015). More recently, studies show that amines, ions and volatile organic vapors can play an important role in NPF events either by participating in the nucleation itself or by stabilizing the nucleated clusters (e.g. Almeida et al., 2013; Berndt et al., 2014; Bianchi et al., 2016; Kirkby et al., 2016). However, several features of atmospheric nucleation, including the actual mechanism in different environments and other possible vapors involved (Kulmala et al., 2006; Lehtinen et al., 2007), remain unknown.

The lack of exact knowledge of atmospheric NPF mechanisms is partly because, at several locations, particle size distribution measurements do not extend to nucleation size range but instead start at ca. 3 nm or even at larger sizes (e.g. 7 or 10 nm). This limits the use of the particle data in NPF studies and poses a challenge in understanding NPF globally. In addition, the actual nucleation rates of sub-2-nm particles remain unknown. Even with data obtained by the new condensation particle counters (CPC), that have cut-off mobility diameters of sub-2 nm (Sgro and Fernández de la Mora, 2004; Iida et al., 2009; Vanhanen et al., 2011; Kuang et al., 2012; Wimmer et al., 2013), the determination of nucleation rates still involves approximation, e.g. due to composition dependent detection efficiencies and high loss rates of the smallest particles.

Measuring sub-3-nm particles is a challenging task because of their diffusion loss during transporting the sample, difficulties in collecting representative samples for electrical detection, difficulties in charging them for electrical size-selection (classification), their insufficient amount to be chemically analyzed, and the need for a very high supersaturation condition to grow them to large enough sizes that they can be optically detected (Kulmala et al., 2012). Because of these challenges in measuring small particles, methods to extrapolate size distributions and formation rates below the measurement range have been suggested by McMurry and Friedlander (1979), McMurry (1982; 1983), Weber et al. (1996); Kerminen and Kulmala (2002); Kerminen et al. (2003); Lehtinen et al. (2007) and most recently by Kürten et al. (2015). We are, however, not aware of another study in which these methods have been tested with atmospheric measurement data.

Our study has two main goals. Firstly, we aim to estimate 3 nm particle formation rates J_3 for Puijo, where continuous size distribution measurements have been going on since 2006. We estimate the J_3 by a scaling method based on aerosol dynamics theory for the range 3 - 7 nm, because the measured size range at Puijo has been only down to 7 nm in diameter. Therefore, our second main goal is to validate our method to estimate J_3. For this, we use size distributions measured at Hyytiälä, where detailed particle size distribution measurements down to 3 nm have been performed since 1996. From the Hyytiälä data we can thus evaluate formation rates both at 3 nm and 7 nm. The fraction of particles that survives the scavenging by larger aerosols is determined by the ratio of their growth and scavenging rates (Kerminen et al., 2004b). In this study, we use the method of Lehtinen et al. (2007) in which time and size independent particle growth rate and, time independent but size dependent coagulation sink are assumed.

2 Methods

2.1 Data sets and site descriptions

In this study we use the aerosol size distribution measurements at two different SMEAR (Station for Measuring Ecosystem-Atmosphere Relations) stations in Finland: SMEAR II located in Hyytiälä and SMEAR IV in Kuopio. SMEAR II (Hyytiälä, southern Finland; 61°51´ N, 24°17´ E, 181 m a.s.l.) is characterized by boreal coniferous forest. The main pollution sources are the city of Tampere (60 km away) and the buildings at the station. These sources are most effective when the wind is from the southwest direction (Kulmala et al., 2001). For this study we analyzed aerosol size distributions measured at SMEAR II with a Differential Mobility Particle Sizer (DMPS; Aalto et al., 2001), with a cut-off size at 3 nm, between years 2000-2012.

At SMEAR IV the instruments are set up at the top of the Puijo observation tower (62°54′34″ N, 27°39′19″ E), 306 m and 224 m above the sea level and the surrounding lake level, respectively). Puijo tower is located in the city of Kuopio (Eastern Finland), a semi-urban environment with surroundings characterized by forest with conifer and deciduous (mostly birch) trees, and many lakes. The main local sources surrounding the tower are a paper mill (direction 35°, distance >1.4 km), the city center (direction 120-155°, distance 1.6-3.2 km), a heating plant (direction 160°, distance 3.5 km), a highway and residential areas (see Leskinen et al. (2009) and Portin et al. (2014) for more details). The aerosol size distribution is measured with a twin-DMPS (Winklmayr et al., 1991; Jokinen and Mäkelä, 1997) covering the size range 7-800 nm (Leskinen et al., 2009). The twin-DMPS consists of two differential mobility analyzer (DMA) tubes, one shorter with 11-cm length and another one longer with 28-cm length, and a condensation particle counter (TSI Model 3010 CPC) after each DMA tube. In both DMPS systems, the sample is neutralized (before it enters to the DMA) into charge equilibrium by a beta radiation source (Ni-63 10 mCi=370 MBq). The size range measured by the longer tube is 27-800 nm with 29 discrete bins and 7-49 nm with 17 discrete bins for the shorter tube. The full particle size distribution (7-800 nm) is measured every 12 minutes (Leskinen et al., 2009). At Puijo there is a twin-inlet system for aerosol-cloud interaction studies: one inlet removes cloud droplets (when the station is in a cloud) and collects only the interstitial particles and the other inlet collects the total aerosol, i.e. cloud droplets and interstitial particles. When the station is not in a cloud, the size distribution measured from both inlets are the same. In this study, we used the data from the total aerosol inlet and analyzed aerosol size distributions measured between April 2007 and December 2015.

2.2 Data analysis method

Kerminen and Kulmala (2002) derived an analytical formula which links the “real” particle formation rate and the “apparent” formation rates of particles of larger sizes for which measurements are available (typically above 3 nm). The formula was later improved by Lehtinen et al. (2007) by (1) correcting the slightly inaccurate size dependence of the coagulation sink, and (2) removing the unnecessary assumption of the identity of the condensing vapor. According to the formula (equation (7) in

Lehtinen et al., 2007) one can estimate the formation rate of smaller particles (J_{d1}) with diameter d_1, for which no measurements are available, from the formation rate of measured larger particles (J_{d2}) with diameter d_2, as follows:

$$J_{d1} = J_{d2} \cdot \exp\left(\gamma \cdot d_1 \cdot \frac{CoagS(d_1)}{GR}\right), \quad (1)$$

with $\gamma = \frac{1}{m+1}\left(\left(\frac{d_2}{d_1}\right)^{m+1} - 1\right)$ and $m = \frac{\log[CoagS(d_2)/CoagS(d_1)]}{log[d_2/d_1]}$,

where *CoagS* is the coagulation sink of smaller particles (diameter d_1) onto the background particles, and *GR* is the particle growth rate (which is assumed to be constant from diameter d_1 to diameter d_2).

In this study, we apply the Eq. (1) to estimate the apparent formation rates of particles of 3 nm in diameter at Puijo where the size distribution of particles below 7 nm is not measured. To derive Eq. (1) (i.e. equation (7) in Lehtinen et al., 2007), it was assumed that the growth rate between d_1 and d_2 is constant. This assumption, however can fail especially for sizes below 3 nm, where some recent studies have indicated strong size dependence of *GR* (Kuang et al., 2012; Kulmala et al., 2013).

Korhonen et al. (2014) modified Eq. (1) to also include either linear or power-law type size dependent growth rate and tested the method by using modelled NPF events. In their studies especially the method assuming power-law type growth rate gave promising results with various types of size dependent growth profiles. However, in this study, we assume a constant *GR* because as mentioned earlier a strong size-dependency of *GR* has been reported for very small particles typically below 3 nm (e.g. Kuang et al., 2012) rather than for larger sizes. The other assumption when deriving Eq. (1) is that the nucleating particles are lost only by coagulation onto larger pre-existing particles. Lehtinen et al. (2003) studied the contribution of particles of different sizes to the condensation sink at Hyytiälä and found that particles below 50 nm in diameter have typically negligible contribution. This is a reasonable assumption at Puijo also as the concentrations and size distributions are similar to those at Hyytiälä. The mean values of CoagS of 7 nm particles are 5.41×10^{-5} s^{-1} and 5.29×10^{-5} s^{-1} in Hyytiälä (event days during 2002-2012) and Puijo (event days during 2007-2015), respectively.

To evaluate Eq. (1) against measurements, we use the particle size distribution evolution data during nucleation event days from SMEAR II. There the measurements have extended down to 3 nm in diameter, and therefore, one is able to get apparent formation rates at 7 nm (J_7) and at 3 nm (J_3) directly from measurements. We then set d_1 = 3 nm and d_2 = 7 nm in Eq. (1) and calculate $J_{3,obs}$ and $J_{7,obs}$ as outlined in Kulmala et al. (2012) and slightly improved in Vuollekoski et al. (2012). Here we use the subscript *obs* to indicate *observed* apparent formation rates *J*. The formation rate of particles of 3 nm ($J_{3,obs}$) and 7 nm ($J_{7,obs}$) in diameter from measured aerosol size distribution were calculated as follows:

$$J_{3,obs} = \frac{dN_{3-7}}{dt} + n_7 . GR_{7-20}, + N_{3-7} . CoagS(d_{GMD}), \quad (2)$$

where $n_7 = \frac{N_{5-9}}{9-5}$ and $d_{GMD} = \sqrt{3 \times 7}$ nm.

$$J_{7,obs} = \frac{dN_{7-10}}{dt} + n_{10} . GR_{7-20} + N_{7-10} . CoagS(d_{GMD}), \quad (3)$$

where $n_{10} = \frac{N_{8-12}}{12-8}$ and $d_{GMD} = \sqrt{7 \times 10}$ nm.

Here $N_{3-7,}$ N_{5-9}, N_{7-10} and N_{8-12} are the number concentration of particles within size ranges 3-7 nm, 5-9 nm, 7-10 nm and 8-12 nm, respectively, and n_7 and n_{10} are the size distribution function at 3 nm and 7 nm, respectively. The coagulation sink (*CoagS*) terms were calculated directly from the measured particle size distributions, taking into account the hygroscopicity effects using the parametrization of Laakso et al. (2004) who used the hygroscopic growth factor parametrization by Zhou (2001). We used a parabolic differentiation method on the measured number concentration to obtain its time-derivative (the first term in Eq. (2) and Eq. (3)). The method fits a second order polynomial to seven data points centered at the data point where derivative is calculated while at the edges a parabola is fit through the first or last six data points, from which the derivative is calculated directly. Also, to avoid spurious fluctuations in the second and third terms in equations 2 and 3, the N_{3-7}, N_{5-9}, N_{7-10} and N_{8-12} were smoothed using a moving average (over five data points) filter.

The estimated formation rate J_3 was then calculated based on Eq. (1):

$$J_{3,est}(t) = J_{7,obs}(t') . \exp\left(\gamma(t).3nm.\frac{CoagS(d_1=3nm)}{GR_{3-10}}\right), \quad (4)$$

Note $J_{3,est}$ at time *t* is calculated based on $J_{7,obs}$ at time t', where $t = t' - \frac{4nm}{GR_{3-10}}$, thus accounting for the growth time of the 3 nm particles to 7 nm particles. To average over this time interval needed for growth, the *m* and $CoagS(d_1)$ values are calculated as medians of the corresponding values during time *t* to t'.

To determine the growth rates required in this study, we used the maximum-concentration method (Lehtinen et al., 2003; Yli-Juuti et al., 2011). In this method, the particle growth rates are determined from the times of the concentration maxima in each of the size-bins of the measured particle number size distributions. A linear function is fitted to the data points of the geometric mean diameters of the size-bins as function of the determined times of the concentration maxima in the size-bins, and the growth rate GR is the slope of this linear function. We also tested another GR determination method, which uses log-normal mode-fitting of the measured size distributions to follow the growth of the particles (Yli-Juuti et al., 2011). However, when

comparing in Hyytiälä the observed 3 nm particle formation rates to those estimated using GR from both maximum-concentration and mode-fitting methods, it become apparent that the maximum-concentration method yielded better results. Therefore, we chose to use the GR from maximum-concentration method in Equations 2, 3 and 4. We left out the days where the growth rates required in the aforementioned equations (i.e. GR_{3-10} and/or $GR_{7\text{-}20}$) were not quantifiable. We chose the size range 3-10 nm rather than 3-7 nm to determine the GR in the exponential term of equation 4 (denoted as GR_{3-10}). This was done to increase the number of data points in the *GR* fitting and thereby to improve the reliability of the fitted *GR*.

After evaluating the analysis method with SMEAR II data, we applied the method for Puijo where the DMPS detection range extended only down to 7 nm. To estimate the formation rate of 3-nm particles at Puijo we adapted Eq. (4) by replacing GR_{3-10} with GR_{7-20} due to lack of DMPS measurements below 7 nm. However, as it will be shown in section 3.1, using GR_{7-20} instead of GR_{3-10} does not affect the accuracy of estimated J_3 for NPF events in Hyytiälä, which is an indication that the size dependence of the growth rate in the range 3-20 nm is typically weak. The $J_{7,obs}$ was calculated with the same method as was used for Hyytiälä (i.e. using equation 3).

3 Results and discussion

3.1 Analysis of estimated J_3 in Hyytiälä (Finland)

Figure 1 shows the comparison of estimated formation rates $J_{3,est}$ (Eq. (4)) with the observed ones $J_{3,obs}$, as calculated directly from the measured size distribution evolution according to Eq. (2) in Hyytiälä. In the top figures, the range 3-10 nm is used to evaluate the growth rate, in the bottom ones 7-20 nm. We analyzed 65 NPF event days for which the formation and growth rates could be quantified. Each data point in Figures 1-b and 1-d represents the arithmetic mean of the 3-nm particle formation rates ($J_{3,est}$ and $J_{3,obs}$) for a single NPF day during the time window from 07:00 to 19:00 local time. The mean is also a measure of the total particle production strength of each event. The results show that, when using GR in the range 3-10 nm, the estimated mean $J_{3,est}$ values correlate with $J_{3,obs}$ with a correlation coefficient of 0.90 and a slope of 0.90 using bilinear fitting. Furthermore, 91 % of estimated $J_{3,est}$ are within a factor of two of the observed $J_{3,obs}$. The corresponding numbers when using GR in the range 7-20 nm are 0.92, 0.87 and 93%. Equation (4) seems to have a tendency of slightly overestimating the formation rate of 3-nm particles. There is not much difference in the results with different GR size ranges. The total means of $J_{3,obs}$ and $J_{3,est}$ (not shown in the figure) calculated using $GR_{3\text{-}10}$ are 0.57 and 0.61 $cm^{-3}\ s^{-1}$, respectively, confirming the tendency of Eq. (4) in slightly overestimating the 3-nm particle formation rates.

One interesting and important result is that there is not much difference in the estimated formation rates with different GR size ranges. This is both an indication of the weak size independence of GR as well as an encouragement for using GR for the size

interval 7-20 nm for Puijo to extrapolate J below 7 nm. The correlation coefficient and the fraction of points within a factor of two for the mean formation rates even increase (from 0.90 to 0.92 and from 91% to 93%, respectively) – however, the regression slope decreases from 0.90 to 0.87.

Figure 1-a and 1-c show $J_{3,obs}$ versus $J_{3,est}$ values with the same 10-minute temporal resolution as for the measured size distribution. The points are within the time window from 07:00 to 19:00 local time. With this higher temporal resolution $J_{3,obs}$ and $J_{3,est}$ are clearly correlated (with correlation coefficients of 0.83 and 0.85 for the $GR_{3\text{-}10}$ and $GR_{7\text{-}20}$ cases, respectively) but the match is not as good as for their daily mean values presented in Figure 1-b. For the time resolved data 58% (60% for the $GR_{7\text{-}20}$ case) of the estimated $J_{3,est}$ are within a factor of two of the observed $J_{3,obs}$. There are three key reasons for this: 1) there are significant fluctuations in time resolved experimental size distribution data, 2) the extrapolation method assumes a constant value for CoagS/GR, and 3) there is a time lag between J_3 and J_7 and a poor estimation of the growth rate *GR* results in comparing values at different times. The variation of CoagS with time also affects *m* and γ in equation 1. This is, however, negligible as CoagS(7 nm)/CoagS(3 nm) is a very weak function of time.

Figure 2 shows examples of the time evolution of the particle size distribution, the different formation rates J and CoagS (3nm) on three NPF days in Hyytiälä. For most of the NPF days (81% of the days) the estimated time-dependence of $J_{3,est}$ (or time-lag between 3-nm and 7-nm particle formation rates) is within one hour of the observed $J_{3,obs}$, and the values of $J_{3,est}$ are in fairly-good agreement with $J_{3,obs}$ (see e.g. Figure 2-d). However, the time-dependency of $J_{3,est}$ is not consistent with $J_{3,obs}$ for some of the days (19% of the days have larger than one hour time difference between $J_{3,est}$ and $J_{3,obs}$) and, instead, typically the $J_{3,est}$ peak occurs earlier than the $J_{3,obs}$ peak (see e.g. Figure 2-e). This indicates that our method of estimating *GR* is not always perfect and underestimates the *GR* values. Figure 2-f shows an example of a NPF day for which the $J_{3,est}$ and $J_{3,obs}$ are dramatically different. This is due to the burst in the number concentration which appeared mostly within the size range 3-7 nm (chosen to calculate $J_{3,obs}$) and is thus not included in the size range 7-10 nm from which $J_{7,obs}$ is calculated and then scaled to $J_{3,est}$. Therefore, Eq. 4 can give quite inaccurate results for NPF days associated with e.g. this type of inhomogeneity in the particle number concentrations in different size ranges. This is one of the general problems when analyzing events measured at one fixed location. We do not observe the same aerosol growing, but particles formed at various location appear at the measurement site at various stages of their growth. If we have a large enough homogeneous region of similar formation and growth, there is no problem. However, if there are inhomogenities and the air mass transport direction changes during an event, we see dynamics as in fig. 2c and f. It can be also concluded that visual inspection of the data is still valuable - cases like this are very challenging for automatic data analysis routines.

3.2 Estimation of J_3 in Puijo (Finland)

For the aerosol size distribution data in Puijo, the NPF event days were first recognized visually and classified as "quantifiable" and "non-quantifiable" based on whether or not the event is homogeneous enough to allow quantification of the basic characteristics such as formation and growth rates (Dal Maso et al., 2005). Therefore, our data pool consists of event (E), non-event (NE) and undefined days, the last being days during which the evolution of the size distribution is too unclear for definitive determination of whether or not NPF has been occurring. Figure 3 shows typical examples of the size distribution dynamics on undefined and NPF days in Puijo. We noticed that there are two types of undefined days in Puijo. One is characterized with a burst in the number concentration of particles of the smallest detectable sizes but doesn't seem to show the characteristics of a NPF event day (i.e. growth to larger sizes, see e.g. Figure 3-a) and most likely originate from local emissions. In the other type, some particles appear in larger sizes (with minor growth), which may or may not be originated from NPF processes (see e.g Figure 3-b). A clear NPF event with particle growth continuing several hours into the evening is shown in Figure 3-c.

The monthly number and yearly fraction of NPF event days recorded in Puijo from year 2007 to 2015 are shown in Figure 4. Note that size distribution data for 48 and 44% of the days are missing during years 2010 and 2012, respectively. Figure 4 shows that a maximum number of event days occurred during spring time similar to NPF events reported in Hyytiälä (Dal Maso et al., 2005). There are 105 quantifiable NPF event days for which we calculated the $J_{3,est}$ at Puijo. Figure 5 shows the seasonal mean values of $J_{3,est}$ and $J_{7,obs}$, GR_{7-20} and coagulation sink for 7-nm particles (*CoagS(d=7 nm)*) for the quantifiable NPF event days in Puijo. The total mean of $J_{3,est}$ is 0.61 , while the corresponding values for $J_{7,obs}$ is 0.44 $cm^{-3}s^{-1}$, respectively. Total means of GR_{7-20} and *CoagS* of 7-nm particles for NPF days are 5.8 nm/h and 1.84×10^{-4} s^{-1}, respectively. Thus, the mean *GR* at Puijo is somewhat higher compared to Hyytiälä where median value of *GR* = 4.3 nm/h is reported for the period April 2003- December 2009 (Yli-Juuti et al., 2011). As the growth rates in Puijo are on average higher, there is less time needed for the particles to grow from 3 to 7 nm. This means that our assumption of time independent growth rate and coagulation sink during growth should hold in Puijo as well as in Hyytiälä.

Table 1 summarizes the seasonal means of parameters presented in Figure 5. The seasonal mean 3-nm particle formation rates seem to have the highest values during summer (1.12 cm^{-3} s^{-1} for 17 NPF days) and spring (0.70 cm^{-3} s^{-1} for 68 NPF days) and drops significantly in fall and winter. The seasonal mean of the growth rate has its maximum in summer (8.0 nm/h) and minimum in winter (2.3 nm/h). The seasonal mean of *CoagS* values for 7 nm during NPF event days are highest in summer and lowest in winter in Puijo.

4 Conclusions

In this study, the formation rates of 3-nm particles in SMEAR IV, Puijo (Finland) were estimated. The measurements at Puijo extend only down to 7 nm in diameter, which means that we had to extrapolate to 3 nm using aerosol dynamics theory. The approach used here is based on the competing processes of condensational growth and scavenging onto background aerosols, assuming time and size independent growth rate and time independent coagulation sink in the range 3 to 7 nm.

To first evaluate our extrapolation method, we applied it to particle formation events at Hyytiälä, where DMPS measurements extend down to 3 nm and formation rates at 3 nm ($J_{3,obs}$) and 7 nm ($J_{7,obs}$) can thus be determined directly from the measured size distribution evolution. The results show that the estimated daily mean values of J_3 are in reasonably good agreement with observed mean J_3, with 91% of the estimated J_3 within a factor of two from the measured ones and, mostly overestimated. However, when considering detailed daily time evolution, the agreement is not as good. This is caused by three main things. First, there are significant fluctuations in experimental size distribution data due to e.g. changes in the sampled airmasses. This kind of fluctuations are not taken into account in Eq. 1. Second, the extrapolation method assumes a constant value for CoagS/GR. If this is not the case, it affects both the time evolution (determined by GR) and the magnitude of the estimated J (determined by the ratio CoagS/GR). Third, there is a time lag between J_3 and J_7, and a poor estimation of the growth rate results in comparing values at different times. Estimating $GR_{3\text{-}10}$, as was shown from Hyytiälä data, does not seem to give in all cases satisfactory results for this purpose. It should be noted that we have to estimate *GR* from the data above 7 nm for Puijo site due to the lack of the measured data below 7 nm.

At Puijo, the mean of J_7 for quantifiable particle formation days was 0.44 $cm^{-3}s^{-1}$, while the extrapolated mean J_3 was 0.61 $cm^{-3}s^{-1}$. These are about two times greater than the corresponding values in Hyytiälä. The ultimate aim of this work was to predict nucleation rates from size distribution measurements that do not extend to sizes lower than 7nm. The results obtained in this study suggest this is very challenging, in large part due to the difficulty in reliably predicting the growth rate down to around 1.5nm. It is noted that the possible size dependence of this growth rate further complicates the matter.

Acknowledgments:

We gratefully acknowledge the financial support by the Academy of Finland Center of Excellence program (project numbers 272041, 1118615, 307331), the Nordic Centre of Excellence CRAICC, University of Eastern Finland (UEF) strategic funding, and ACTRIS (under the European Union Seventh Framework Programme (FP7/2007–2013) grant agreement no. 262254 and Horizon 2020 research and innovation programme under grant agreement no. 654109) and Academy of Finland (project number 299544).

References

Aalto, P., Hämeri, K., Becker, E., Weber, R., Salm, J., Mäkelä, J., Hoell, C., O'dowd, C., Hansson, H.-C., Väkevä, M., Koponen, I., Buzorius, G., and Kulmala, M.: Physical characterization of aerosol particles during nucleation events, Tellus B [Online], Volume 53, 2001.

Asmi, E., Kivekäs, N., Kerminen, V.-M., Komppula, M., Hyvärinen, A.-P., Hatakka, J., Viisanen, Y., and Lihavainen, H.: Secondary new particle formation in Northern Finland Pallas site between the years 2000 and 2010, Atmos. Chem. Phys., 11, 12959-12972, doi:10.5194/acp-11-12959-2011, 2011.

Almeida, J., Schobesberger, S., Kürten, A., Ortega, I. K., Kupiainen-Määttä, O., Praplan, A. P., Adamov, A., Amorim, A., Bianchi, F., Breitenlechner, M., David, A., Dommen, J., Donahue, N. M., Downard, A., Dunne, E., Duplissy, J., Ehrhart, S., Flagan, R. C., Franchin, A., Guida, R., Hakala, J., Hansel, A., Heinritzi, M., Henschel, H., Jokinen, T., Junninen, H., Kajos, M., Kangasluoma, J., Keskinen, H., Kupc, A., Kurtén, T., Kvashin, A. N., Laaksonen, A., Lehtipalo, K., Leiminger, M., Leppä, J., Loukonen, V., Makhmutov, V., Mathot, S., McGrath, M. J., Nieminen, T., Olenius, T., Onnela, A., Petäjä, T., Riccobono, F., Riipinen, I., Rissanen, M., Rondo, L., Ruuskanen, T., Santos, F. D., Sarnela, N., Schallhart, S., Schnitzhofer, R., Seinfeld, J. H., Simon, M., Sipilä, M., Stozhkov, Y., Stratmann, F., Tomé, A., Tröstl, J., Tsagkogeorgas, G., Vaattovaara, P., Viisanen, Y., Virtanen, A., Vrtala, A., Wagner, P. E., Weingartner, E., Wex, H., Williamson, C., Wimmer, D., Ye, P., Yli-Juuti, T., Carslaw, K. S., Kulmala, M., Curtius, J., Baltensperger, U., Worsnop, D. R., Vehkamäki, H., and Kirkby, J: Molecular understanding of sulphuric acid-amine particle nucleation in the atmosphere. Nature, 502: 359-363, doi:10.1038/nature12663, 2013.

Berndt, T., Sipilä, M., Stratmann, F., Petäjä, T., Vanhanen, J., Mikkilä, J., Patokoski, J., Taipale, R., Mauldin III, R. L., and Kulmala, M.: Enhancement of atmospheric H_2SO_4 / H_2O nucleation: organic oxidation products versus amines, Atmos. Chem. Phys., 14, 751-764, doi:10.5194/acp-14-751-2014, 2014.

Bianchi, F., Tröstl, J., Junninen, H., Frege, C., Henne, S., Hoyle, C.,R., Molteni, U.,Herrmann, E., Adamov, A., Bukowiecki, N., Chen, X., Duplissy, J., Gysel, M., Hutterli, M., Kangasluoma, J., Kontkanen, J., Kürten, A., Manninen, H. E., Münch, S., Peräkylä, O., Petäjä, T., Rondo, L., Williamson, C., Weingartner, E., Curtius, J., Worsnop, D. R., Kulmala, M., Dommen, J., and Baltensperger, U.: New particle formation in the free troposphere: A question of chemistry and timing. Science 352, 1109-1112, 2016. DOI: 10.1126/science.aad5456

Dal Maso, M., Kulmala, M., Riipinen, I., Wagner, R., Hussein, T., Aalto, P. P. & Lehtinen K. E. J.: Formation and growth of fresh atmospheric aerosols: eight years of aerosol size distribution data from SMEAR II, Hyytiälä, Finland, Boreal Environment Research. 10, 5, p. 323-336. 14 p, 2005.

Fuzzi, S., Baltensperger, U., Carslaw, K., Decesari, S., Denier van der Gon, H., Facchini, M. C., Fowler, D., Koren, I., Langford, B., Lohmann, U., Nemitz, E., Pandis, S., Riipinen, I., Rudich, Y., Schaap, M., Slowik, J. G., Spracklen, D. V., Vignati, E., Wild, M., Williams, M., and Gilardoni, S.: Particulate matter, air quality and climate: lessons learned and future needs, Atmos. Chem. Phys., 15, 8217-8299, doi:10.5194/acp-15-8217-2015, 2015.

Hussein, T., Dal Maso, M., Petäjä, T., Koponen, I. K., Paatero, P., Aalto, P. P., Hämeri, K. & Kulmala, M.: Evaluation of an automatic algorithm for fitting the particle number size distributions. Boreal Env. Res. 10: 337–355, 2005.

Iida, K., Stolzenburg, M. R., McMurry, P. H.: Effect of Working Fluid on Sub-2 nm Particle Detection with a Laminar Flow Ultrafine Condensation Particle Counter, Aerosol Science and Technology, 43:1, 81-96, doi: 10.1080/02786820802488194, 2009.

Jokinen, V. and Mäkelä, J. M.: Closed-loop arrangement with critical orifice for DMA sheath/excess flow system, J. Aerosol Sci., 28, 643–648, 1997.

Kerminen, V.-M., & Kulmala, M.: Analytical formulae connecting the "real" and the "apparent" 25 nucleation rate and the nuclei number concentration for atmospheric nucleation events. Journal of Aerosol Science, 33, 609–622, doi: http://dx.doi.org/10.1016/S0021-8502(01)00194-X, 2002.

Kerminen, V.-M., Lehtinen, K. E. J., Anttila, T. and Kulmala, M.: Dynamics of atmospheric nucleation mode particles: a timescale analysis. Tellus B, 56, 135-146, doi: 10.1111/j.1600-0889.2004.00095.x, 2003.

Kerminen, V.-M., Anttila, T., Lehtinen, K. E. J. and Kulmala, M.: Parameterization for atmospheric new-particle formation: Application to a system involving sulfuric acid and condensable water-soluble organic vapors, Aerosol Sci. Tech. 38, 1001-1008, doi: 10.1080/027868290519085, 2004.

Kerminen, V.-M., Paramonov, M., Anttila, T., Riipinen, I., Fountoukis, C., Korhonen, H., Asmi, E., Laakso, L., Lihavainen, H., Swietlicki, E., Svenningsson, B., Asmi, A., Pandis, S. N., Kulmala, M., and Petäjä, T.: Cloud condensation nuclei production associated with atmospheric nucleation: a synthesis based on existing literature and new results, Atmos. Chem. Phys., 12, 12037-12059, doi:10.5194/acp-12-12037-2012, 2012.

Kirkby, J., Duplissy, J., Sengupta, K., Frege, C., Gordon, H., Williamson, C., Heinritzi, M., Simon, M., Yan, C., Almeida, J., Tröstl, J., Nieminen, T., Ortega, I. K., Wagner, R., Adamov, A., Amorim, A., Bernhammer, A.-K., Bianchi, F., Breitenlechner, M., Brilke, S., Chen, X., Craven, J., Dias, A., Ehrhart, S., Flagan, R. C., Franchin, A., Fuchs, C., Guida, R., Hakala, J., Hoyle, C. R. , Jokinen, T., Junninen, H., Kangasluoma, J., Kim, J., Krapf, M., Kürten, A., Laaksonen, A., Lehtipalo, K., Makhmutov, V., Mathot, S., Molteni, U., Onnela, A., Peräkylä, O., Piel, F., Petäjä, T., Praplan, A. P. , Pringle, K., Rap, A., Richards, N. A. D., Riipinen, I., Rissanen, M. P. , Rondo, L., Sarnela, N., Schobesberger, S., Scott, C. E. , Seinfeld, J. H., Sipilä, M., Steiner, G., Stozhkov, Y., Stratmann, F., Tomé, A., Virtanen, A., Vogel, A. L., Wagner, A., Wagner, P. E., Weingartner, E., Wimmer, D., Winkler, P. M., Ye, P., Zhang, X., Hansel, A., Dommen, J., Donahue, N. M., Worsnop, D. R., Baltensperger, U., Kulmala, M., Carslaw, K. S., Curtius, J.: Ion-induced nucleation of pure biogenic particles, Nature, doi:10.1038/nature12663, 2016.

Korhonen, P., Kulmala, M., Laaksonen, A., Viisanen, Y., McGraw, R. and Seinfeld, J. H.: Ternary nucleation of H2SO4, NH3, and H2O in the atmosphere,Journal of Geophysical Research: Atmospheres,104, 26349—26353, doi = 10.1029/1999JD900784,1999.

Korhonen, H., Kerminen,V. M., Kokkola, H., and Lehtinen, K. E. J.: Estimating atmospheric nucleation rates from size distribution measurements: Analytical equations for the case of size dependent growth rates, Journal of Aerosol Science, 69, 13-20, doi:http://dx.doi.org/10.1016/j.jaerosci.2013.11.006, 2014.

Kuang, C., Chen, M., McMurry, P. H., and Wang, J.: Modification of laminar flow ultrafine condensation particle counters for the enhanced detection of 1 nm condensation nuclei, Aerosol Sci. Technol., 46, 309–315, 2012.

Kürten, A., Williamson, C., Almeida, J., Kirkby, J., and Curtius, J.: On the derivation of particle nucleation rates from experimental formation rates, Atmos. Chem. Phys., 15, 4063-4075, doi:10.5194/acp-15-4063-2015, 2015.

Kulmala, M., Liisa, P, and Mäkelä, J. M.: Stable sulphate clusters as a source of new atmospheric particles, Nature 404, no. 6773, 66-69, doi: 10.1038/35003550, 2000.

Kulmala M., Hämeri K., Aalto P. P., Mäkelä J. M., Pirjola L., Nilsson E. D., Buzorius G., Rannik Ü., Maso M. D., Seidl W., Hoffman T., Janson R., Hansson H.-C., Viisanen Y., Laaksonen A. & O'Dowd C. D.: Overview of the international project on biogenic aerosol formation in the boreal forest (BIOFOR). Tellus B, 53: 324–343. doi: 10.1034/j.1600-0889.2001.530402, 2001.

Kulmala, M., Vehkamäki, H., Petäjä, T., Dal Maso, M., Lauri, A., Kerminen, V.-M., Birmili, and W., McMurry, P.H.: Formation and growth rates of ultrafine atmospheric particles: a review of observations, J Aerosol Sci., 35:143-76, doi:10.1016/j.jaerosci.2003.10.003, 2004.

Kulmala, M., Lehtinen, K. E. J., and Laaksonen, A.: Cluster activation theory as an explanation of the linear dependence between formation rate of 3 nm particles and sulphuric acid concentration, Atmos. Chem. Phys., 6, 787–793, doi:10.5194/acp-6-787-2006, 2006.

Kulmala, M., Petäjä, T., Nieminen, T., Sipilä, M., Manninen, H. E, Lehtipalo, K., Dal Maso, M., Aalto, P. P, Junninen, H., Paasonen, P., Riipinen, I., Lehtinen, K. E J, Laaksonen, A., Kerminen, V.-M.: Measurement of the nucleation of atmospheric aerosol particles, 7, 1651–1667, doi: http://dx.doi.org/10.1038/nprot.2012.091, 2012.

Kulmala, M., Kontkanen, J., Junninen, H., Lehtipalo, K., Manninen, H. E., Nieminen, T., Petäjä, T., Sipilä, M., Schobesberger, S., Rantala, P., Franchin, A., Jokinen, T., Järvinen, E., Äijälä, M., Kangasluoma, J., Hakala, J., Aalto, P. P., Paasonen, P., Mikkilä, J., Vanhanen, J., Aalto, J., Hakola, H., Makkonen, U., Ruuskanen, T., Mauldin, R. L., Duplissy, J., Vehkamäki, H., Bäck, J., Kortelainen, A., Riipinen, I., Kurten, T., Johnston, M. V., Smith, J. N., Ehn, M., Mentel, T. F., Lehtinen, K. E. J., Laaksonen, A., Kerminen, V.-M., Worsnop, D. R.: Direct Observations of Atmospheric Aerosol Nucleation, 339, 943—946, doi: 10.1126/science.1227385, 2013.

Laakso, L., Petäjä, T., Lehtinen, K. E. J., Kulmala, M., Paatero, J., Hõrrak, U., Tammet, H., and Joutsensaari, J.: Ion production rate in a boreal forest based on ion, particle and radiation measurements, Atmos. Chem. Phys., 4, 1933-1943, doi:10.5194/acp-4-1933-2004, 2004.

Laaksonen, A., Kulmala, M., Berndt, T., Stratmann, F., Mikkonen, S., Ruuskanen, A., Lehtinen, K. E. J., Dal Maso, M., Aalto, P., Petäjä, T., Riipinen, I., Sihto, S.-L., Janson, R., Arnold, F., Hanke, M., Ücker, J., Umann, B., Sellegri, K., O'Dowd, C. D., and Viisanen, Y.: SO_2oxidation products other than H_2SO_4 as a trigger of new particle formation. Part 2: Comparison of ambient and laboratory measurements, and atmospheric implications, Atmos. Chem. Phys., 8, 7255-7264, doi:10.5194/acp-8-7255-2008, 2008.

Lehtinen, K. E. J. and Kulmala, M.: A model for particle formation and growth in the atmosphere with molecular resolution in size. Atmos. Chem. Phys. 3, 251-257, 2003.

Lehtinen, K. E. J., Korhonen, H., Dal Maso, M. and Kulmala, M.: On the concept of condensation sink diameter. Boreal Env. Res. 8, 405-411, 2003.

Lehtinen, K. E. J., dal Maso, M., Kulmala, M., and Kerminen, V.- M.: Estimating nucleation rates from apparent particle formation rates and vice versa: Revised formulation of the Kerminen–Kulmala equation, J. Aerosol Sci., 38, 988–994, 2007.

Leskinen, A., Portin, H., Komppula, M., Miettinen, P., Arola, A., Lihavainen, H., Hatakka, J., Laaksonen, A., Lehtinen, K. E. J.: Overview of the research activities and results at Puijo semiurban measurement station, Boreal Env. Res., 14, 576–590, 2009.

McMurry, P. H., and S. K. Friedlander: New particle formation in the presence of an aerosol, Atmos. Environ., 13, 1635 – 1651, 1979.

McMurry, P. H., & Wilson, J. C.: Growth laws for the formation of secondary ambient aerosols: Implications for chemical conversion mechanisms. Atmospheric Environment (1967), 16(1), 121-134. doi:10.1016/0004-6981(82)90319-5, 1982.

McMurry, P. H.: New particle formation in the presence of an aerosol: Rates, time scales and sub-0.01 mm size distributions, J. Colloid Interface Sci., 95(1), 72 – 80, 1983.

Merikanto, J., Spracklen, D. V., Mann, G. W., Pickering, S. J., and Carslaw, K. S.: Impact of nucleation on global CCN, Atmos. Chem. Phys., 9, 8601-8616, doi:10.5194/acp-9-8601-2009, 2009.

Minguillón, M. C., Brines, M., Pérez, N., Reche, C., Pandolfi, M., Fonseca, A. S., Amato, F., Alastuey, A., Lyasota, A., Codina, B., Lee, H.-K., Eun, H.-R. , Ahn, K.-H. , Querol, X.: New particle formation at ground level and in the vertical column over the Barcelona area, Atmospheric Research, Volumes 164–165, Pages 118-130, doi:10.1016/j.atmosres.2015.05.003, 2015.

Nie, W., Ding, A., Wang, T., Kerminen, V.-M., George, C., Xue, L., Wang, W., Zhang, Q., Petäjä, T., Qi, X., Gao, X., Wang, X., Yang, X., Fu, C., Kulmala, M.: Polluted dust promotes new particle formation and growth, 4, 6634, doi:10.1038/srep06634, 2014.

Portin, H., Leskinen, A., Hao, L., Kortelainen, A., Miettinen, P., Jaatinen, A., Laaksonen, A., Lehtinen, K. E. J., Romakkaniemi, S., and Komppula, M.: The effect of local sources on particle size and chemical composition and their role in aerosol–cloud interactions at Puijo measurement station, Atmos. Chem. Phys., 14, 6021-6034, doi:10.5194/acp-14-6021-2014, 2014.

Sgro , L. A., Fernández de la Mora, J.: A Simple Turbulent Mixing CNC for Charged Particle Detection Down to 1.2 nm, 38, 1-11, 10.1080/02786820490247560, 2004.

Vanhanen, J., Mikkilä, J., Lehtipalo, K., Sipilä, M., Manninen, H. E., Siivola, E., Petäjä, T., Kulmala., M.: Particle Size Magnifier for Nano-CN Detection, Aerosol Science and Technology, 45:4, 533-542, 2011.

Vuollekoski, H., Sihto, S.-L., Kerminen, V.-M., Kulmala, M., and Lehtinen, K. E. J.: A numerical comparison of different methods for determining the particle formation rate, Atmos. Chem. Phys., 12, 2289-2295, doi:10.5194/acp-12-2289-2012, 2012.

Weber, R. J., McMurry, P. H., Eisele, F. L. , Tanner, D. J.: Measurement of Expected Nucleation Precursor Species and 3–500-nm Diameter Particles at Mauna Loa Observatory, Hawaii, Journal of the Atmospheric Sciences 1995 52:12, 2242-2257, 1995.

Weber, R. J., Marti, J. J., and McMurry, P. H., Eisele, F. L., Tanner, D. J., and Jefferson, A.: Measured atmospheric new particle formation rates: implications for nucleation mechanisms, Chemical Engineering Communications, 151, 53-64, doi: 10.1080/00986449608936541, 1996.

Wimmer, D., Lehtipalo, K., Franchin, A., Kangasluoma, J., Kreissl, F., Kürten, A., Kupc, A., Metzger, A., Mikkilä, J., Petäjä, T., Riccobono, F., Vanhanen, J., Kulmala, M., and Curtius, J.: Performance of diethylene glycol-based particle counters in the sub-3 nm size range, Atmos. Meas. Tech., 6, 1793–1804, doi:10.5194/amt-6-1793-2013, 2013.

Winklmayr, W., Reischl, G. P., Linder, A. O., and Berner, A.: A new electromobility spectrometer for the measurement of aerosol size distribution in the size range 1 to 1000 nm, J. Aerosol Sci., 22, 289–296, 1991.

Yli-Juuti, T., Nieminen, T., Hirsikko, A., Aalto, P. P., Asmi, E., Hõrrak, U., Manninen, H. E., Patokoski, J., Dal Maso, M., Petäjä, T., Rinne, J., Kulmala, M., and Riipinen, I.: Growth rates of nucleation mode particles in Hyytiälä during 2003−2009: variation with particle size, season, data analysis method and ambient conditions, Atmos. Chem. Phys., 11, 12865-12886, doi:10.5194/acp-11-12865-2011, 2011.

Xiao, S., Wang, M. Y., Yao, L., Kulmala, M., Zhou, B., Yang, X., Chen, J. M., Wang, D. F., Fu, Q. Y., Worsnop, D. R., and Wang, L.: Strong atmospheric new particle formation in winter in urban Shanghai, China, Atmos. Chem. Phys., 15, 1769-1781, doi:10.5194/acp-15-1769-2015, 2015.

Zhou, J.: Hygroscopic Properties of Atmospheric Aerosol Particles in Various Environments, PhD thesis, University of Lund, Division of Nuclear Physics, Sweden, http://lup.lub.lu.se/record/41435, 2001.

Table 1. Overall and seasonal mean values of the observed formation rates of 7-nm particles ($J_{7,obs}$), the estimated formation rates of 3-nm particles ($J_{3,est}$), the growth rates of particles in size range 7-20 nm (GR_{7-20}) and the coagulation sink of 7 nm particles onto larger particles ($CoagS_7$) for 105 NPF days which occurred at Puijo during Apr 2007 - Dec 2015. The $J_{7,obs}$, $J_{3,est}$ and $CoagS_7$ include data during 07:00–19:00 on each NPF day.

	$J_{7,obs}$ ($cm^{-3}\ s^{-1}$)	$J_{3,est}$ ($cm^{-3}\ s^{-1}$)	GR_{7-20} (nm/h)	$CoagS_7$ (s^{-1})
Winter (Dec-Feb)	0.16	0.22	4.3	1.4×10^{-4}
Spring (Mar-May)	0.49	0.70	5.0	1.9×10^{-4}
Summer (Jun-Aug)	0.85	1.12	8.0	2.3×10^{-4}
Fall (Sep-Nov)	0.27	0.40	5.7	1.7×10^{-4}
Overall	0.44	0.61	5.8	1.8×10^{-4}

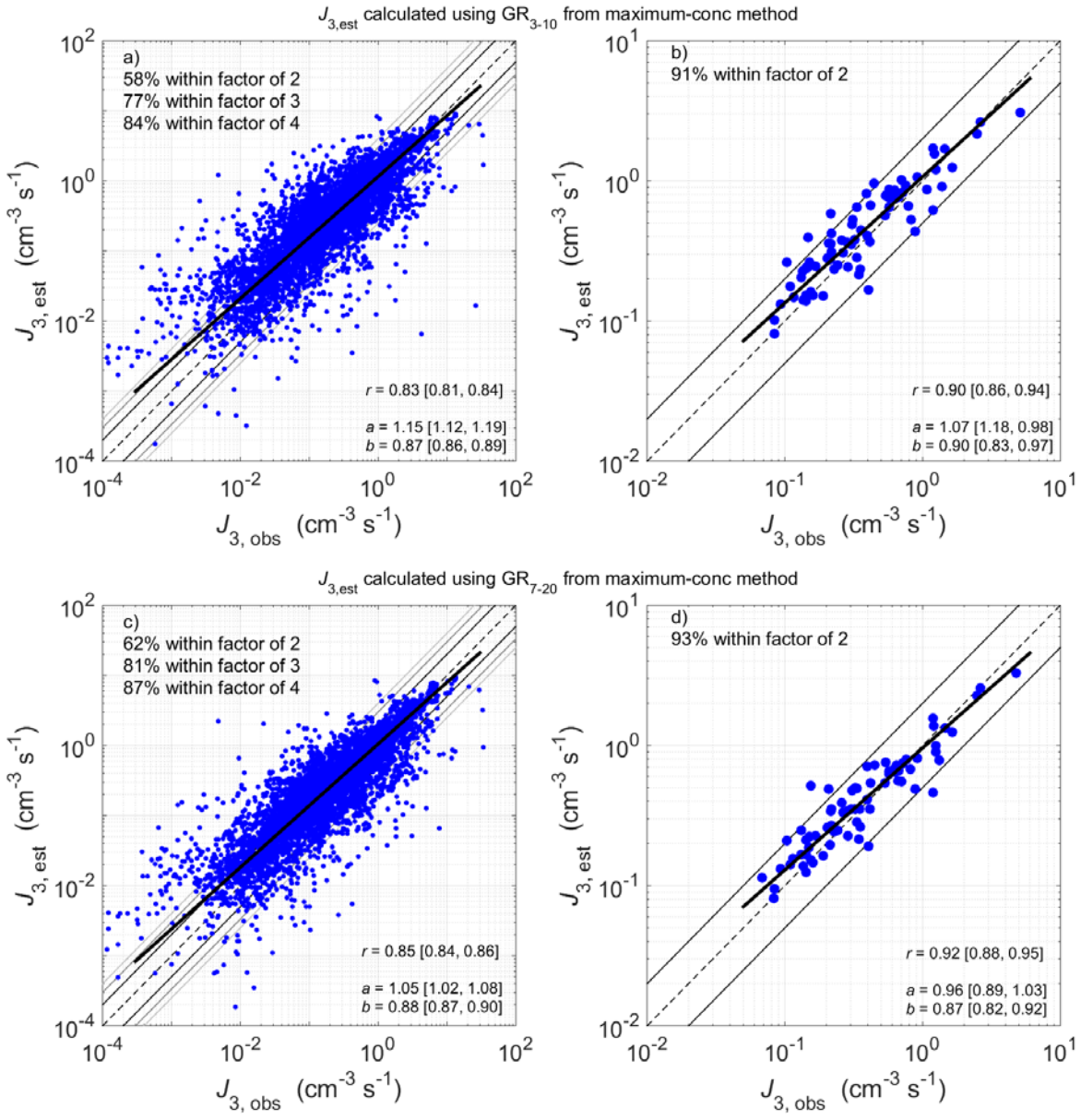

Figure 1. Comparison of the estimated ($J_{3,est}$) against observed ($J_{3,obs}$) formation rates of 3 nm particles during the selected new-particle formation (NPF) event days in Hyytiälä. Panels a), c) show formation rates $J_{3,est}$ and $J_{3,obs}$ calculated at 10-minute time resolution between 7:00–19:00. Note that the time-lag during which particles grow from 3 nm to 7 nm is taken into account in the $J_{3,est}$. Panels b), d) show arithmetic mean of formation rates between 07:00 to 19:00 local time for each NPF day. Panels in the top row refer to $J_{3,est}$ results calculated using GR_{3-10}, and the bottom row to those calculated using GR_{7-20}. The black lines show the bivariate linear fits to the logarithmic data values; the corresponding parameter values of the fit

equations $J_{3,est} = a \cdot J_{3,obs}^{b}$ and the correlation coefficients r are given in each panel. The values in square brackets show the 5th and 95th percentile bootstrap confidence intervals of the parameter values. The fractions of J3,est that are within factor of 2 of J3,obs are shown in the upper left corner of each subplot (for the 10-minute time resolution data also data points within fraction of 3 and 4 are shown).

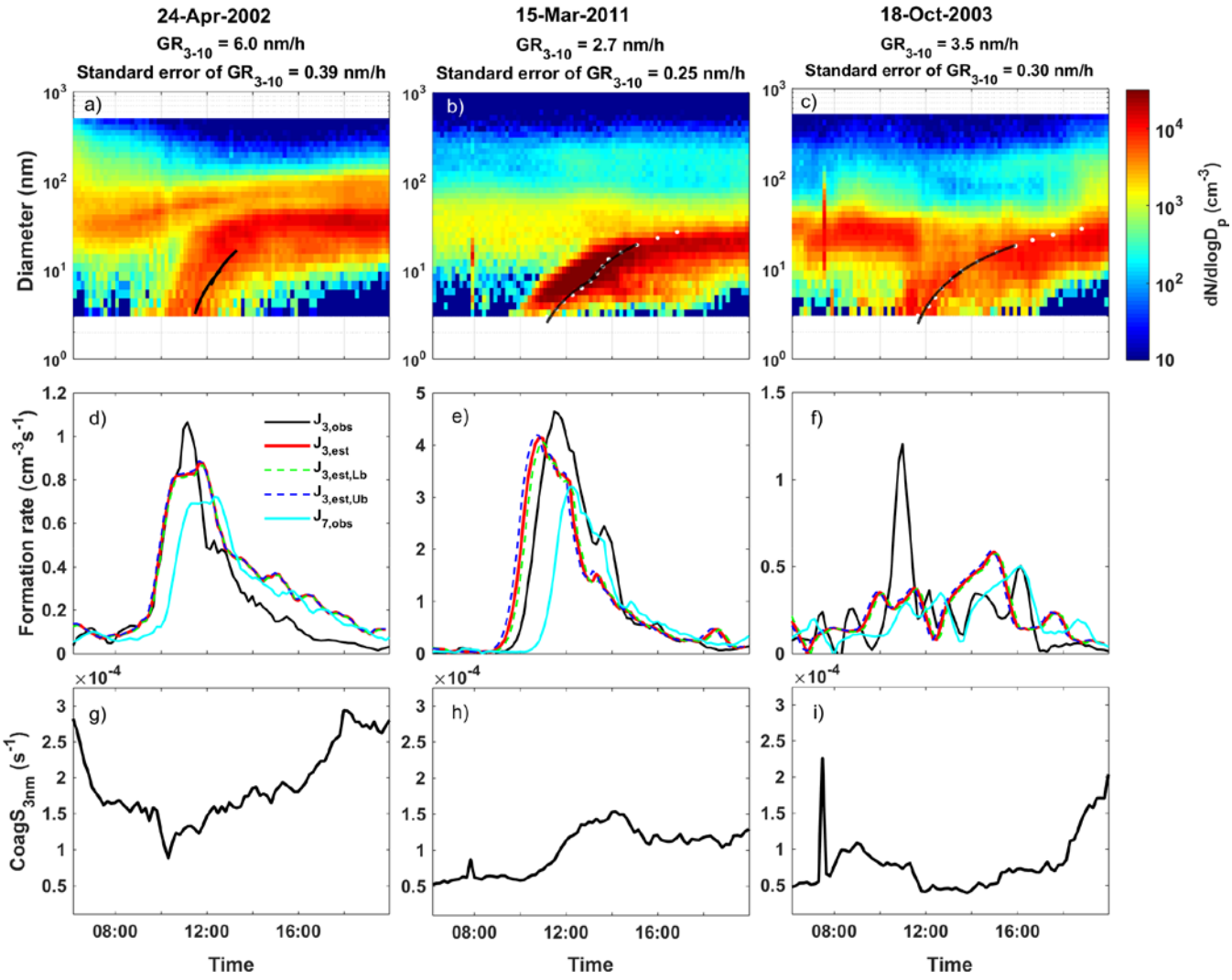

Figure 2. Examples of Hyytiälä NPF events. a, b, and c) the evolution of the particle number size distribution. White dots represent the times of the maximum concentration in each size-bin of the measured size distribution, and the solid black line shows the first-order polynomial fit to those data points. Figures d), e) and f) are the corresponding time-evolution of 3 nm particle formation rates $J_{3,obs}$ obtained from Eq. (2) (black line), observed formation rates of 7 nm particles $J_{7,obs}$ obtained from Eq. (3) (cyan line), and the estimated formation rate of 3 nm particles $J_{3,est}$ calculated by Eq. (4) (red line). The dashed lines show the upper bound ($J_{3,est,Ub}$) and lower bound ($J_{3,est,Lb}$) calculated by Eq. (4) using the lower ($GR_{3–10}$ - SE) and upper ($GR_{3–10}$ + SE) bound of $GR_{3–10}$, respectively. Figures g), h) and i) show the time evolution of the coagulation sink of 3 nm particles.

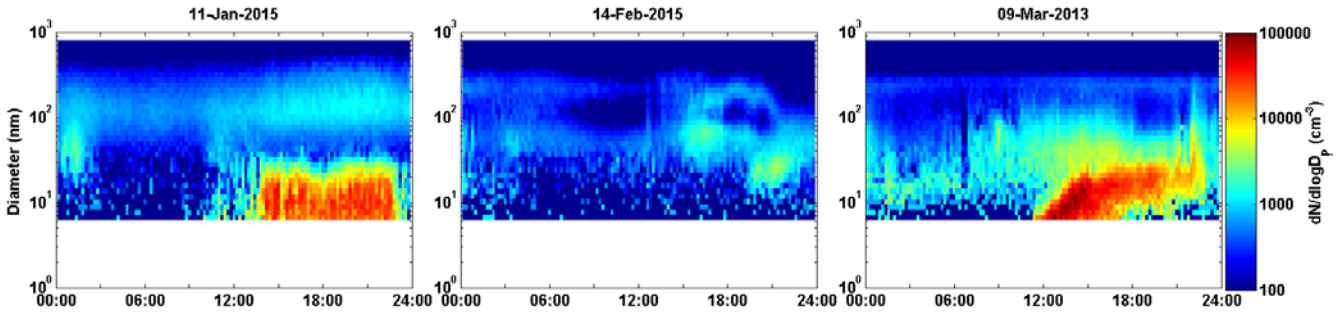

Figure 3. Examples of the time evolution of the aerosol size distribution in Puijo for (a) an undefined day characterized by a burst in the number concentrations of the small particles which doesn't have the characteristics of a typical NPF event day (b) a typical undefined day, and (c) a clear NPF event day.

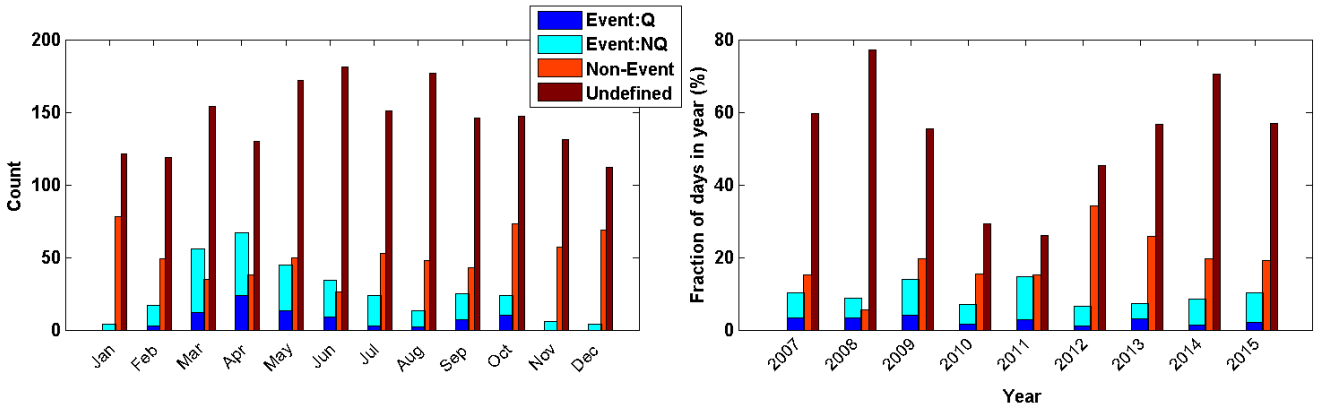

Figure 4. Monthly number (left panel) and yearly fraction (right panel) of NPF event days (divided into Quantifiable Events (Q) and Non-Quantifiable events (NQ)), Non-Events (NE) and undefined days recorded in Puijo during period 2007-2015. Fraction of (e.g. NE) days in year is the ratio of number of NEs and number of days within the year. Note that the days for which bad or no data were recorded are not shown here. Note that 48 and 44% of the days are missing during years 2010 and 2012, respectively.

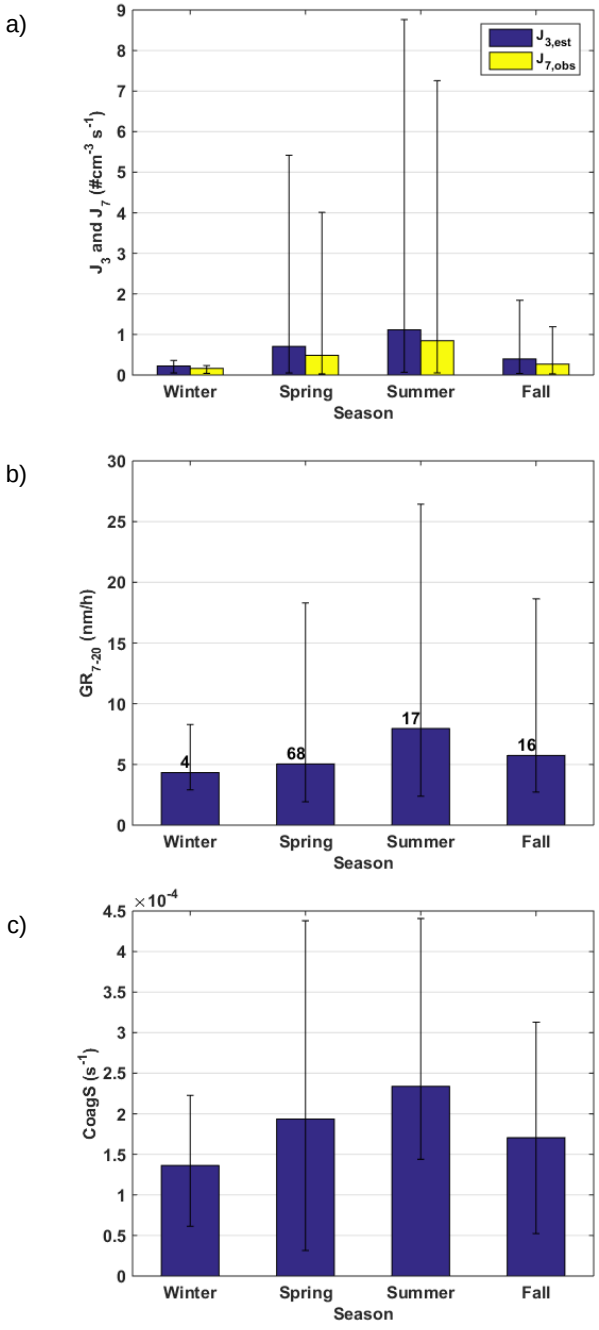

Figure 5. Seasonal mean values of different parameters for NPF days at Puijo: a) estimated formation rates of 3-nm particles ($J_{3,est}$) and observed formation rates of 7-nm particles ($J_{7,obs}$). b) growth rate of the particles within size range 7-20 nm c) coagulation sink (*CoagS*) of 7-nm particles. The height of the bars shows the mean values of data points (i.e. mean values

during 7:00 to 19:00 of the *J* and *CoagS* values for 105 NPF event days) within each season, and the error bars indicate the values between minimum and maximum of the data points. The numbers on top of each bar in middle panel indicate the number of the NPF events in corresponding season. The same applies to the Figures 5-a and 5-c.